Absorption Currents and Voltages in Ceramic Capacitors with Cracks

Alexander Teverovsky

***Abstract* - Measurement of insulation resistance (IR) in multilayer ceramic capacitors (MLCCs) is considered a screening technique that assures the dielectric is free of defects. This work analyzes the effectiveness of this technique for revealing cracks in ceramic capacitors. It is shown that absorption currents prevail over leakage currents during standard IR measurements. Absorption currents, and consequently IR, have a weak temperature dependence, increasing linearly with voltage (before saturation), and are not sensitive to the presence of mechanical defects. In contrary, intrinsic leakage currents increase super-linearly with voltage and exponentially with temperature (activation energy is in the range from 0.6 eV to 1.1 eV). Leakage currents associated with the presence of cracks have a weaker dependence on temperature and voltage compared to the intrinsic leakage currents. For this reason, intrinsic leakage currents prevail at high temperatures and voltages, thus masking the presence of defects. A simple model that is based on the Dow equivalent circuit for capacitors with absorption has been developed to assess the resistance of capacitors at low voltages and room temperature conditions. Comparative analysis of long-term (up to several hundreds of hours) variations of absorption voltages in normal capacitors and capacitors with cracks has been carried out to evaluate IR at low voltages and assess the effectiveness of absorption voltage measurements in revealing capacitors with cracks.**

***Index Terms:* ceramic capacitor, leakage current, insulation resistance, dielectric absorption, cracks.**

I. INTRODUCTION

MLCCs constitute the majority of components used in electronic assemblies. Most of their failures are related to cracks that are caused either by insufficient process control during manufacturing, thermal shock associated with soldering, or flex cracking during handling and/or mechanical testing of the circuit boards. These cracks, if not identified, might cause failures after months and even years of operation. The failure mode varies from a short circuit to intermittent, or "noisy," behavior that in some cases might be misjudged as software failures.

Two screening procedures that are used during the manufacturing of MLCCs are often considered sensitive to the presence of defects in the dielectric: measurements of the dielectric withstanding voltage (DWV) and measurements of the insulation resistance (IR). Our previous work [1] analyzed the effectiveness of DWV screening to reveal capacitors with cracks, and this study is focused on the effectiveness of IR measurements.

Currents in MLCCs decrease with time relatively slowly after voltage step applications. Also, when such a capacitor is left disconnected after a brief short circuit period, the voltage across the electrodes increases with time. This behavior is due to polarization processes in the dielectric that might include dipole orientation, redistribution of ionic charges, charge injection from electrodes, or electron tunneling into the traps in the dielectric [2]. Disregarding the specific physical mechanism of polarization, a slow (from seconds to hours) decrease of currents with time can be described as a process of charge absorption. An increase in voltage across a disconnected capacitor, after a brief short circuit period, is also due to absorbed charges that are released back to the electrodes. Currents and voltages related to these processes are defined as absorption currents and absorption voltages (AV), respectively. The first includes polarization currents under poling conditions and depolarization currents under short circuit conditions. In technical literature, the phenomenon of voltage recovery is often referred to as the dielectric absorption (DA).

Absorption processes are well known in a variety of dielectric materials employed in different types of capacitors, including MLCCs [3-5]. Absorption currents typically follow the empirical Curie van Schwendler law, referred to as a Kohlrausch behavior in some publications [6]. According to this law, polarization currents decrease with time as a power function,

$$I(t) = I_0 \times t^{-n}, \tag{1}$$

where I_0 and n are constants, and n is close to 1.

Absorption voltage depends on the polarization conditions (applied voltage and time of polarization), discharge time, and time of recovery. All of these conditions vary substantially for different applications, and most circuit designers are concerned about the short-term effects of DA [7]. For this reason, the method of DA measurements specified in MIL-PRF-19978 has a limited value, and to some degree can be used to assess only a relative capability of different materials for voltage recovery. Most literature data related to DA were obtained within seconds or minutes after shorting, and there is no information on the long-term behavior of absorption voltages in capacitors.

The purpose of this work is to gain insight into absorption and leakage currents in low-voltage MLCCs, investigate voltage and temperature dependencies of these currents, and assess their sensitivity to the presence of cracks. Modeling of absorption voltages and a comparative analysis of their long-term variations for normal capacitors and capacitors with

To be published in Electrical and Electronics Engineers (IEEE) Transactions on Device and Materials Reliability and on nepp.nasa.gov.

cracks has been carried out in order to evaluate IR of capacitors at low voltages and assess the effectiveness of AV measurements for revealing capacitors with defects.

II. EXPERIMENT

A variety of MLCCs produced by seven different vendors were used in this study to reveal common features in absorption currents and voltages. Most of the parts were commercial high volumetric efficiency X7R capacitors with EIA size variations from 0402 to 2225, voltage rating (VR) from 6.3 V to 100 V, and capacitance from 1500 pF to 100 µF.

Mechanical defects in MLCCs were introduced using three techniques:

- Mechanical fracture. A corner portion of the part was chipped-off using fine cutters.
- Local fracturing. A capacitor was damaged by a hit with a Vickers indenter.
- Thermal shock. Capacitors were stressed by a cold thermal shock using the ice water testing (IWT) technique described in [8] or hot thermal shock using a solder dip test.

These techniques were used to simulate manufacturing or assembly/handling related cracking in ceramic capacitors and have different advantages and drawbacks in approaching this goal. Mechanical fracturing guarantees that internal electrodes are exposed to environments, but the charge transport processes on the cleaved surface might be somewhat different compared to the processes in cracks (water surface adsorption compared to water capillary condensation). Ice water testing forms cracks that are filled with water initially, and baking does not remove water completely. Cracks caused by solder dip testing might be difficult to detect. The indenter causes local damage that provides the closest simulation to the real life cracking, but there is no guarantee that the cracks penetrate deep enough to cross internal electrodes. In all cases described in this work, the presence of cracks crossing the active area of the capacitors was confirmed by additional testing in humid environments.

DC currents and absorption voltages were measured using source-measurement units manufactured by Keithley (model 236) and Agilent (hp4156A). Variations of AV with time were recorded after poling and 5-second shorting of capacitors.

AC characteristics of the parts (capacitance, C, and dissipation factor, DF) were measured using Agilent 4294 precision impedance analyzer at 1 kHz. Only parts with acceptable AC characteristics were used for the following tests. In most cases, fracturing did not cause significant variations of C and/or DF. This suggests that AC characteristics are not sensitive to the presence of cracks.

III. ABSORPTION AND LEAKAGE CURRENTS IN MLCCS

Typical relaxations of currents in various ceramic capacitors after the application of rated voltages are shown in Fig. 1. In double logarithmic coordinates, *I-t* characteristics can be approximated with straight lines over a long period of time, typically from seconds to several hours. This confirms the applicability of the power law Eq.(1). Absorption currents are highly reproducible and measurements on groups of up to 20 samples showed that all parts have the same amplitudes and rate of decay. The currents increased with capacitance and depending on the part type, the exponent n varied in the range from 0.6 to 1.3. For Mfr.C 1 µF 6.3 V capacitors (Fig. 1a), the currents level off after ~ 1 hour due to absorption currents decreasing below the intrinsic leakage currents in the parts. Comparison between polarization and depolarization absorption currents (Fig.1b), showed that in all cases the currents were similar. Analysis of current relaxation in ceramic capacitors with different types of dielectric materials (X7R, X5R, and NPO/COG) confirmed Curie - van Schwendler behavior in all cases.

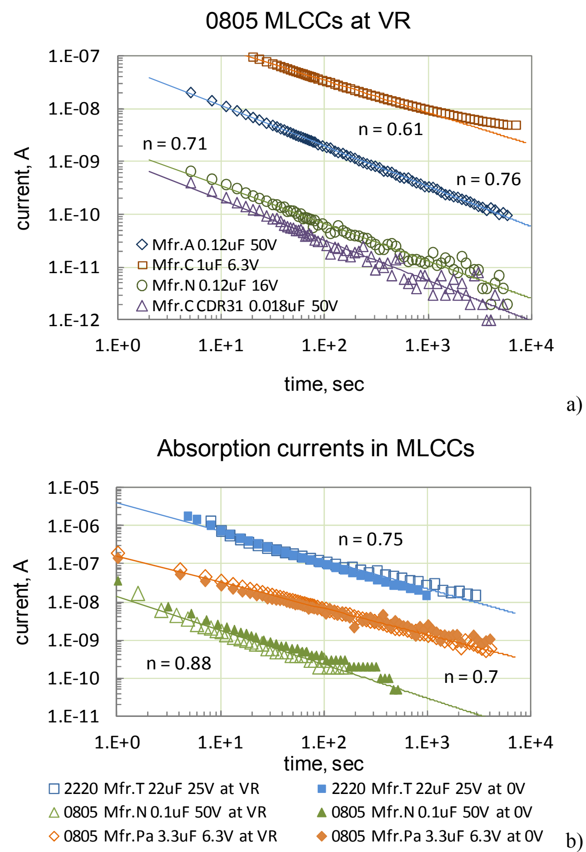

Fig. 1. Polarization currents in four types of 0805 X7R MLCCs from different vendors (a) and comparison of polarization currents measured at rated voltages (empty marks) and depolarization currents (solid marks) in three types of X7R MLCCs.

An increase in applied voltage increases isochronic absorption currents, whereas the rate of current decay that can be characterized by the exponent *n* remains practically the same (see Fig. 2a). At voltages exceeding the rated by 2 to 3 times, the current decay levels-off after 100 to 1000 sec due to increased leakage currents. Absorption currents that were measured after 120 sec of poling (time that is required for IR measurements) are plotted against voltage in Fig. 2b and indicate a linear dependence of I_{120} on voltage. The slope of each line indicates resistance values varying from 2.4×10^{8} Ohm to 1.5×10^{10} Ohm for the capacitors shown in Fig. 2b. These values exceeded the specified IR requirements in all parts.

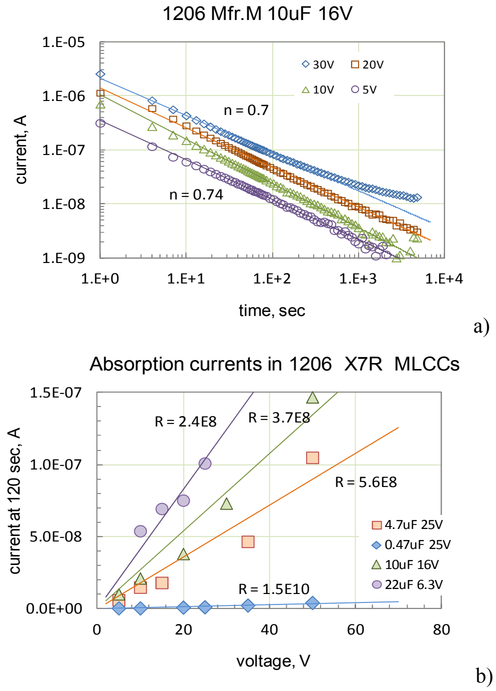

Fig. 2. Absorption currents in 10 µF 16 V capacitors at different voltages (a) and voltage dependence of isochronic currents measured after 120 sec of polarization in five different types of X7R capacitors (see legends).

Variations of absorption and leakage currents with voltage for 3.3 µF 6.3 V capacitors are shown in Fig. 3. The absorption (depolarization) currents increase linearly up to ~ 20 V and then saturate with voltage (see Fig 3b). At voltages exceeding ~ 3VR, leakage currents are significantly greater than absorption currents. Variations of leakage currents with voltage can be approximated with a power law, $I(t) \sim V^{m}$, where the exponent m is a constant close to 5. Additional analysis for this and other parts tested at room temperature showed that plotting leakage currents with voltage in Schottky, $ln(I)$ vs. $V^{0.5}$, Poole-Frenkel, $ln(I/V)$ vs. $V^{0.5}$, and double logarithmic coordinates resulted in equally good linearization of the data (the correlation factor, R2 , exceeded 0.99). Unfortunately, linearization in the relative coordinates does not allow for discrimination of the physical mechanisms (Schottky, Poole-Frenkel, or space charge limited current, SCLC) responsible for conduction in ceramic capacitors.

Examples of I-V characteristics for different types of MLCCs are shown in Fig. 4.

At room temperature, all data, including that for the part shown in Fig. 3, can be approximated with straight lines in Schottky coordinates. However, at high temperatures, a better fit is obtained in double logarithmic coordinates, which suggests that the current is a power function of voltage. The slope of the room temperature *I-V* curves in Schottky coordinates varied from 0.9 $(m/V)^{0.5}$ to 1.1 $(m/V)^{0.5}$. At high temperatures, the exponent m varied in a relatively narrow range, from 1.42 to 1.52. Similar results were obtained for different part types manufactured by different vendors. This indicates that at high temperatures, *I-V* characteristics of most X7R capacitors follow the 3/2 power law.

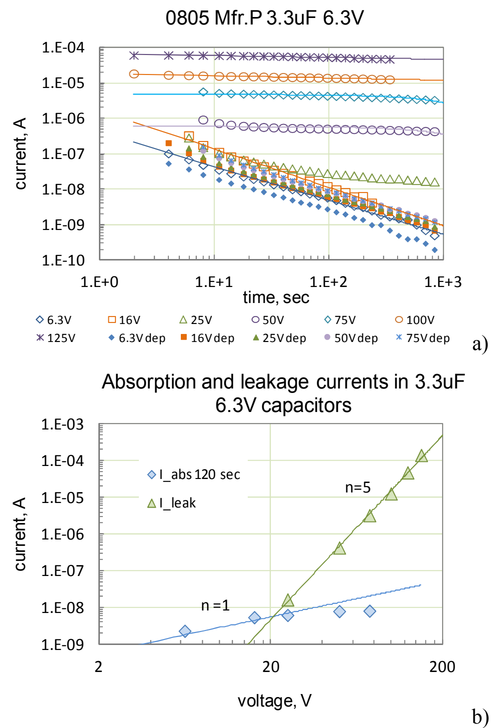

Fig. 3. Time dependence of polarization (empty marks) and depolarization (solid marks) currents in 3.3 µF 6.3 V capacitors at different voltages (a) and voltage dependence of leakage and absorption (120 sec) currents (b).

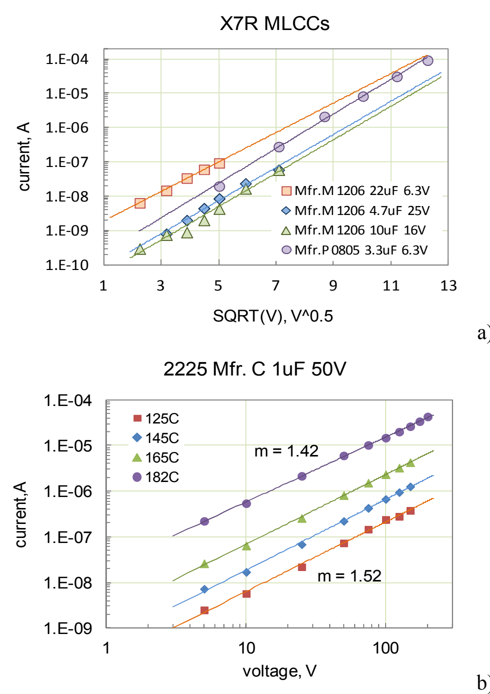

Fig. 4. Room temperature *I-V* characteristics of X7R capacitors in Schottky coordinates (a) and high temperature *I-V* characteristics in double logarithmic coordinates for 1µF 50V capacitors (b).

Measurements of *I-t* characteristics at VR for 47 µF 16 V capacitors at temperatures varying from room (300 K) to cryogenic (200 K and 36 K), showed that the temperature decrease does not change substantially isochronic currents or decay rates (see Fig. 5). Polarization and depolarization currents in different types of 1206 X7R capacitors that were tested in the range from room to 165 °C also did not change substantially with temperature (see example in Fig. 5b). Absorption (depolarization) currents were practically temperature independent, whereas leakage currents dominated at 85 °C and above. Similar results were obtained for other capacitors from different vendors and suggest that absorption currents have a weak dependence on temperature.

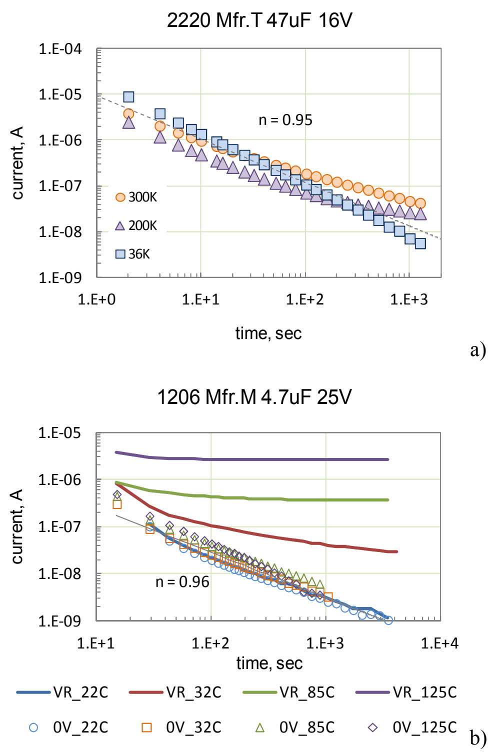

Figure 5. Current relaxation at room and cryogenic temperatures (200 K and 36 K) for 47 µF 16 V capacitors (a) and relaxation of polarization (lines) and depolarization (marks) currents for 4.7 µF 25V 1206 X7R capacitors at temperatures from room to 165 °C (b).

An example of temperature dependencies of leakage currents at different voltages is shown in Fig. 6. In Arrhenius coordinates, the experimental data can be approximated accurately enough with straight lines with slopes indicating the activation energy, E_a. In all cases, the slope decreases as the voltage increases, indicating a decrease in the activation energy (see Fig. 6b.) At relatively low voltages, the activation energy for different part types varies from 0.55 eV to 1 eV and decreases by 10% to 30% as the voltage increases from 5 V to 30 V.

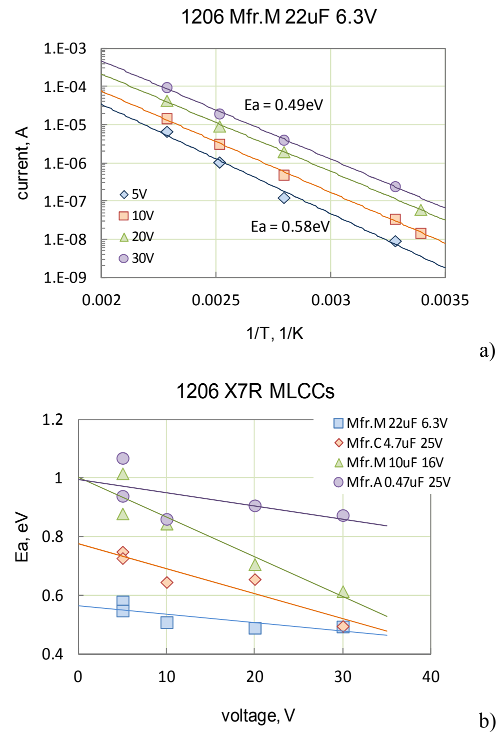

Fig. 6. Temperature dependence of leakage currents at different voltages for 22 µF 6.3V capacitors in Arrhenius coordinates (a) and variation of activation energy with voltage (b).

IV. Effect of Cracking on Absorption and Leakage Currents

I-t characteristics were measured on a variety of normal quality (virgin) ceramic capacitors and capacitors with cracks. In all cases, except for a few with the most severely damaged capacitors, absorption currents (both, polarization and depolarization) were similar for virgin and damaged parts. An example of these measurements at room temperature is shown in Fig. 7a. Fig. 7b shows a close correlation of currents measured after 120 sec in 15 different types of virgin and fractured capacitors. Even in the cases with severely damaged capacitors, leakage currents were below the absorption currents during the first 120 seconds of electrification, meaning that these capacitors would not be detected by the IR screening.

Currents in 15 types of 1206 X7R virgin and fractured capacitors were measured over a wide range of voltages and temperatures, reaching 165 °C. Typical results of these measurements for 22 µF 6.3 V capacitors at 85 °C are shown in Fig. 8. This figure indicates that the increase in temperature does not allow the presence of mechanical defects in MLCCs to be revealed. This is due to a high level of intrinsic leakage currents that exceed the level of currents associated with the presence of cracks.

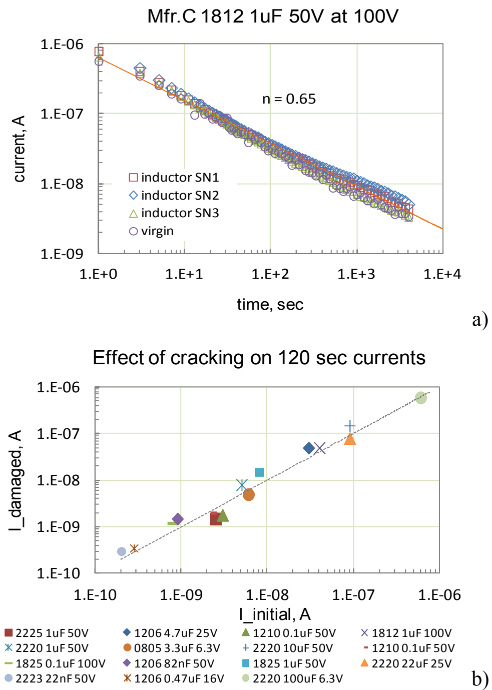

Fig. 7. Relaxation of currents in normal and fractured 1 µF 50V X7R capacitors (a) and the effect of fracturing on the current, measured after 2 min of electrification in different types of X7R capacitors (b).

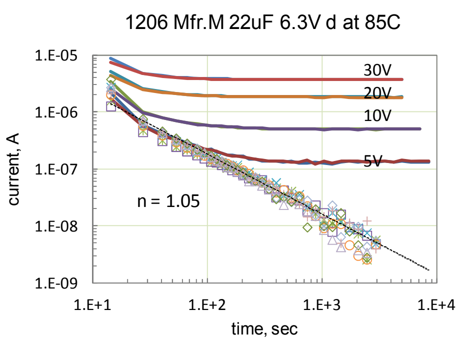

Fig. 8. Polarization (at 5V to 30V) and depolarization (marks) currents in two 22 µF 6.3 V capacitors at 85 °C. Although one of the two parts was damaged with a Vickers indenter and the other was virgin, both had very close currents.

V. Absorption Capacitance

If a charge, Q_t, that is transferred into the dielectric during poling increases with voltage linearly, the absorption process can be described by a capacitance, C_t, that is determined as $C_t = Q_t/V$. The value of Q_t was calculated by approximation of the absorption currents with a power law and integration with time over the period from 1 sec to 10,000 sec.

Variations of the absorption charge with voltage for 10 different types of capacitors are shown in Fig. 9. Results show that Q_t varies linearly up to voltages exceeding the rated voltage by 2 to 3 times. Consequently, the slopes of the lines at relatively low voltages were calculated to estimate values of C_t.

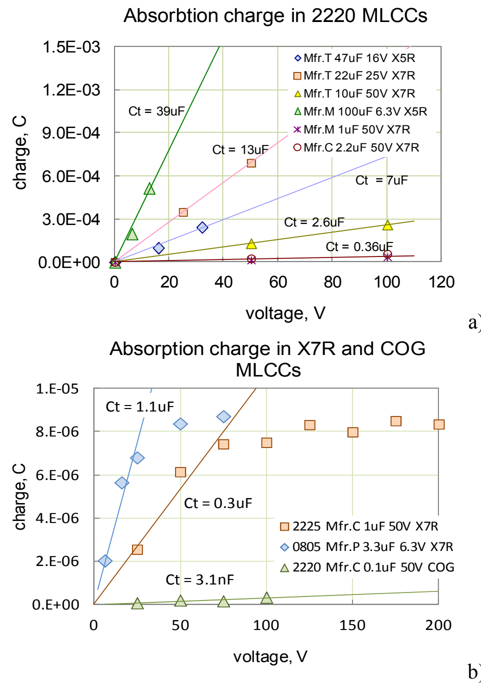

Fig. 9. Variations of absorption charges in different types of X7R/X5R (a) and X7R/COG (b) capacitors calculated by integration of absorption currents with time vs. applied voltage. The absorption capacitance (C_t) was calculated as the slope of $Q_t - V$ lines.

Absorption capacitance is greater for capacitors of larger values and there is a correlation between C_0 and C_t (see Fig. 10). For most tested X7R capacitors, C_t values were in the range from 10% to 50% of the nominal value. On average, $C_t = 0.3\times C_0$. Therefore, the capacitance measured at millihertz frequencies would be on average $1.3\times C_0$. However, for COG capacitors the value of absorption capacitance is much less (see Fig. 9.b) and comprises ~ 3% of C_0.

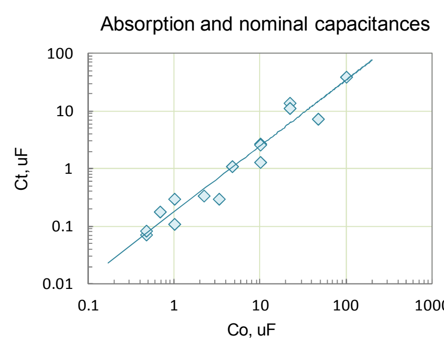

Fig. 10. Correlation between the absorption and nominal values of capacitance for 15 different types of X7R MLCCs.

VI. Modeling of Absorption Currents and Voltages

An equivalent circuit of a capacitor that accounts for the effects related to dielectric absorption was suggested first for polystyrene capacitors by Dow in 1958 [9] and is presented in Fig. 11a. The capacitor has a nominal value C_0 and insulation resistance R. Dow showed that most absorption polarization processes in capacitors can be described using a circuit with five r-C_t relaxators connected in parallel to C_0 by a proper selection of the relaxation times $\tau_i = r_i \times C_{ti}$ and absorption capacitances C_{ti}. If a step voltage V_0 is applied at $t = 0$, than variations of the current with time can be given by a simple equation:

$$I(t) = \frac{V_0}{R} + \sum_i \frac{V_0}{r_i} \exp\left(-t/\tau_i\right) \qquad (2)$$

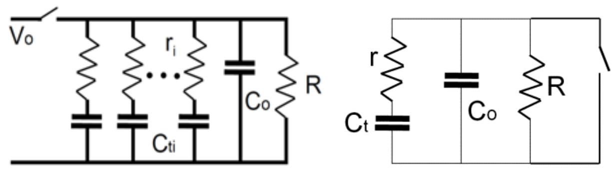

a) b)

Fig. 11. Dow model of a capacitor with absorption (a) and a model for calculations of the absorption voltages (b).

Analysis shows that using the Dow presentation experimental *I-t* characteristics for absorption currents can be modeled accurately enough. The exponent n in the Curie van Schwendler law is equal to 1 for C_{ti} = constant and r_i increases tenfold for each consecutive resistor. Experimental results for capacitors with a relatively slow decay, $n < 1$, can be simulated by increasing C_{ti} for larger r_i, and parts with $n > 1$ by decreasing C_{ti} for larger r_i.

If a capacitor that is modeled by the circuit shown in Fig. 11a remains under bias for a long period of time (exceeding the maximum characteristic time τ_i), then each of the capacitors C_{ti} will be charged to V_0. Shorting for a period of Δt will discharge only C_0, and capacitors C_{ti} associated with relatively fast r_i-C_{ti} relaxators that have $\tau_i < \Delta t$. All other capacitors will remain charged, and when the circuit is open, these charges will leak out to C_0 and increase the voltage across the capacitor. This voltage will increase with time until discharging currents through the leakage resistor R prevail, thus resulting in the voltage roll-off. The absorption voltage, V_{abs}, will decrease with time, and eventually the capacitor will discharge completely. At relatively large insulation resistances and relatively short periods of time after an open circuit occurs, variations of the absorption voltage do not depend on R and the process is not sensitive to the presence of defects in capacitors. However, decreasing V_{abs} with time is controlled by the value of R and for this reason the following analysis is focused on relatively long-term processes occurring during and after the voltage roll-off.

When the absorption voltage is decreasing with time, the process is scaled to the characteristic time related to the insulation resistance R, $\tau_0 = R \times C_0$. By this time, relaxators with $\tau_i << \tau_0$ will be mostly discharged onto C_0. Considering that the charging period is less than τ_0, relaxators with $\tau_i >> \tau_0$ have practically no charge, and will not contribute substantially to the discharging process. For this reason, we can simplify the equivalent circuit by considering only relaxators having timing characteristics τ_i that are close to the duration of polarization.

Let us consider the schematic of the capacitor shown in Fig. 11b that had been pre-charged for some time and then short-circuited briefly. At the end of the pre-charge period, the voltage across capacitor C_t was U_0 and due to a large value of resistor r, it did not change substantially during the short circuit period. For this circuit, variations of the voltage across the capacitor with time can be written in the form:

$$v(t) = A \times \exp(x_1 \times t) + B \times \exp(x_2 \times t), \qquad (3)$$

Constants $x_{1,2}$ are solutions of the relevant characteristic equation:

$$x_{1,2} = \frac{-b \pm \sqrt{b^2 - 4ac}}{2a}$$, where $a = \tau_0 \frac{\tau}{\tau_t}$, $b = \frac{\tau + \tau_t + \tau_0}{\tau_t}$, $c = \frac{1}{\tau_t}$

are constants, and $\tau = r \times C_t$, $\tau_0 = R \times C_0$, $\tau_t = R \times C_t$, are the characteristic times of the charge distribution processes. Constants A and B can be found from the initial conditions:

$v(0) = 0$ and $\left.\frac{dv}{dt}\right|_0 = \frac{U_0}{r \times C_0}$, and can be expressed as follows:

$$A = \frac{U_0}{r \times C_0 \times (x_1 - x_2)}, \quad B = -A.$$

Simulations showed that the time to roll-off and the rate of voltage decrease depend strongly on the value of R and can be used to estimate the insulation resistance of the capacitors.

VII. Effect of Fracturing on Absorption Voltages

A default procedure for absorption voltage, V_{abs}, measurements in our experiments was polarization at *VR* for one hour followed by a 5-sec short-circuit period, after which the voltage across the part was recorded. Examples of absorption voltages are shown in Fig. 12 and indicate a high reproducibility of the measurements from sample to sample. The voltage increases with time during a period that for different part types varies from several hours to several dozens of hours, and then decreases gradually with time. In most cases, the maximum V_{abs} exceeded 1 or 2 volts, and the capacitor remained at voltages above 1 V even after hundreds of hours of storage at room conditions.

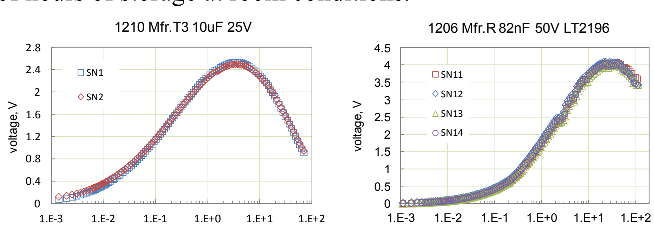

a) b)

Fig. 12. Variations of absorption voltages in two samples of 10 µF 25 V (a) and four samples of 82 nF 50 V (b) X7R capacitors.

Experiments showed that an increase in duration of the polarization period enlarges V_{abs}, and so does an increase in the voltage during polarization. In all cases, there was a trend for saturation of absorption voltages at high levels of polarization. The maximum value of V_{abs} does not correlate with the value of capacitance, and in some cases, absorption voltages as large as 5 to 8 volts were reached after a few hours of storage for capacitors in the nano-farad range.

Time dependence of the absorption voltage is in agreement with the model described in section VI. Dashed lines in the V_{abs} charts shown in Fig. 13 and 14 are calculations per Eq.(3) using the best-fit approximation and parameters adjustment technique. The values of C_t used for calculations were obtained from *I-t* characteristics, as described in section V.

A comparison of absorption voltages in different types of X7R capacitors that are in normal conditions and cracked conditions (introduced by the Vickers indenter) is shown in Fig. 13. In the damaged capacitors, a decrease of V_{abs} occurs much earlier, and the reproducibility of test results is less than that of normal parts. This is obviously due to the uncontrollable level of damage to the parts. For 10 µF 16V capacitors, the calculated resistance dropped from an initial 3×10^{12} Ω to 4×10^{10} Ω after fracture. For 0.1 µF 100V capacitors, IR decreased by 2 to 4 orders of magnitude, from more than 5×10^{14} Ω initially to 2.5×10^{12} Ω - 7×10^{10} Ω for different fractured samples. In all cases, even fractured capacitors had IR exceeding the specified requirements.

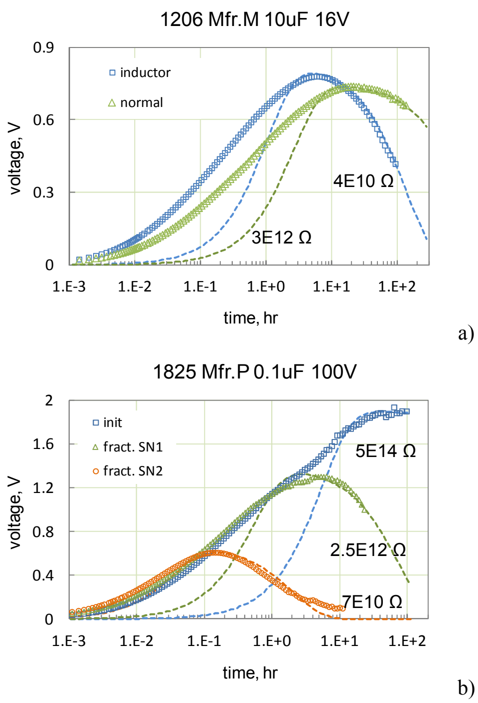

Fig. 13. Absorption voltages in normal and damaged by Vickers indenter 10 µF 16V capacitors (a) and mechanically fractured 0.1 µF 100V (b) X7R capacitors. Dashed lines are calculations per Eq.(2) at indicated values of the insulation resistance.

Two types of thermal shock, the ice water test and the solder dip test, were used to evaluate the effect of cracking on absorption voltages in large-size (EIA 2220) 10 µF 50 V and 1 µF 50 V capacitors. Results of these tests are shown in Fig. 14. For 10 µF capacitors, the initial value of IR was 5×10^{13} ohm and the value after fracture was reduced to 3×10^{10} ohm. The difference was less dramatic for 1 µF capacitors, but still IR decreases an order of magnitude, from 3×10^{12} ohm to 3×10^{11} ohm.

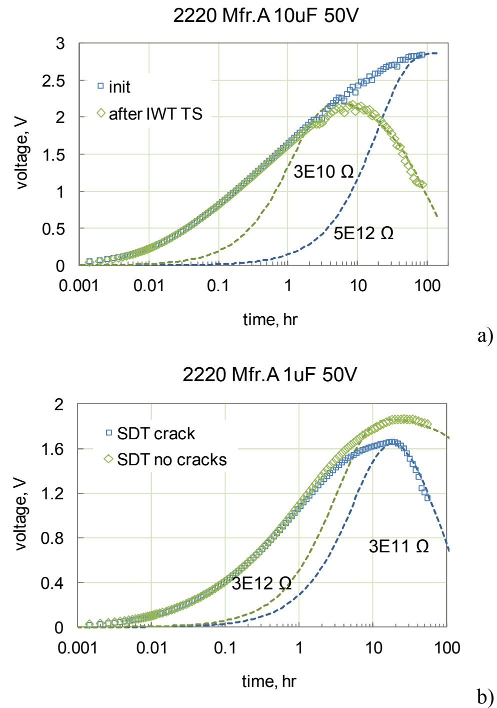

Fig. 14. Effect of the ice water thermal shock on 10 µF 50 V (a) and solder dip thermal shock on 1 µF 50 V X7R capacitors (b).

The effect of fracture on the values of resistance that was calculated based on the measurements of absorption voltages (IR_{abs}) for 20 different part types is shown in Fig. 15. In 70% of the cases, a substantial (more than 2-times) decrease of IR_{abs} was observed. The resistance in capacitors with cracks remained rather large, typically exceeding 10^9 ohm, and was above the specified values for capacitors.

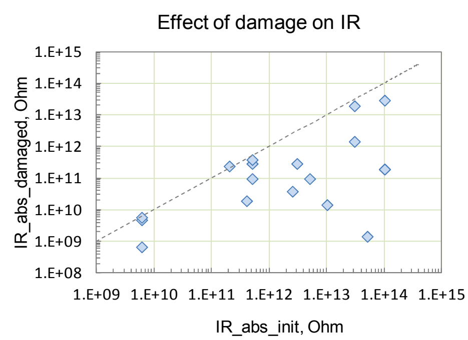

Fig. 15. Effect of fracturing on the value of resistance, calculated based on absorption voltage measurements in 20 X7R capacitors. Dashed line corresponds to no-change values.

VIII. Discussion

Analysis of currents in MLCCs indicates three areas on the *I-t* curves: (1) charging currents, I_{ch}, that prevail typically at times below ~ 1 sec, (2) absorption currents, Iabs, prevailing at times below a few hours, and (3) leakage currents that might be observed at times exceeding a few hours. The latter is a sum of the intrinsic leakage current, I_{il}, that is caused by conduction through the bulk of the dielectric layers, and defect-related leakage current, I_{dl}, that is caused by structural or mechanical defects, like cracks and delaminations. For quality assurance purposes, it is important to assess the defect-related component of the currents. This requires a better understanding of the factors affecting absorption and intrinsic leakage currents.

A. Absorption currents.

Our data show that absorption currents dominate during standard IR measurements, and the leakage currents can only be revealed after hours of polarization. At relatively low voltages, typically below 2-3 times VR, I_{abs} increases with voltage linearly and practically does not depend on temperature. Short circuit (depolarization) currents flow in the opposite direction but have the same isochronic values as polarization currents. These facts are consistent with literature data [2, 10] and can be explained assuming that the absorption process is due to the tunneling of electrons from electrodes into states (traps) located in the forbidden energy gap of the dielectric interface with the metal electrodes. Traps with different energy levels have different probabilities of trapping, which results in substantial (exponential) variations of the characteristic times of the process. For uniformly distributed traps, the characteristic times would change by orders of magnitude, which is consistent with the Dow model. Different distributions of the trap density with energy result in variations of the exponent in the Curie van-Schvendler law.

A close location of the traps to electrodes (likely within dozens of angstroms) results in most of the trapped charges flowing back to the electrodes under shorting conditions, and hence in the reversibility of the absorption process. Charges that are trapped within the bulk of the dielectric will be emptied towards both electrodes, resulting in a negligible current in the external circuit. A saturation of absorption currents at high voltages, that was observed in several cases, is due to the traps filling up and can be used to assess their concentration, N_t, that can be estimated based on measurements of the absorption capacitance. It has been shown in section V that C_t is proportional to the value of the nominal capacitance, $C_t = \alpha \times C_0$, where α is a constant that is close to 0.3 at voltages up to ~ 3VR. In this case:

$$C_t = \frac{q \times N_t \times S}{3 \times VR} = \alpha \frac{\varepsilon \times \varepsilon_0 \times S}{d}, \qquad (4)$$

where d is the thickness of the dielectric, S is the surface area of electrodes, ε is the dielectric constant of the dielectric, $q = 1.6\times10^{-19}$ C is the electron's charge, and $\varepsilon_0 = 8.89\times10^{-14}$ F/cm is the dielectric constant of vacuum. From Eq.(4) the value of N_t can be calculated as:

$$N_t = 3\alpha \frac{\varepsilon \times \varepsilon_0 \times VR}{d \times q}. \qquad (5)$$

Assuming that for a typical X7R capacitor VR is in the range from 6 V to 50 V, d from 5 μm to 15 μm, and $\varepsilon = 3000$, N_t is in the range from 1.8×10^{13} cm^{-2} to 6×10^{13} cm^{-2}.

B. Intrinsic leakage currents.

Contrary to the absorption currents, intrinsic leakage currents increase with voltage super-linearly. Therefore, at sufficiently high voltages (typically exceeding VR) these currents dominate the total current through a capacitor after a few seconds of polarization.

Ceramic materials used in MLCCs are good insulators, and it has been established that their conduction is related to electrons injected from metal electrodes [5]. However, there is no agreement in literature on the mechanism of electron transport. The mechanism of conduction through ferroelectric materials was attributed to the electrode-limited Schottky emission [11-13], bulk-limited Poole-Frenkel transport [14-15], or space charge limited conduction, SCLC [10, 16].

The Schottky equation is applicable to systems with a mean free path of electrons that is greater than the thickness of the dielectric, which is not valid for MLCCs. It has been shown [17] that for ferroelectric thin films, the corrected form suggested by Simmons [18] provides a better agreement with experimental data. According to Simmons, for insulators having small electronic mean free paths, a modified equation can be written as:

$$J_S = AT^{3/2}\mu E \exp\left(-\frac{\Phi_B}{kT}\right)\exp\left(\frac{\beta_s E^{0.5}}{kT}\right), \qquad (6)$$

where A = 3.08×10^{-4} A/cm^2_K$^{1.5}$ is the constant, μ is the electron mobility in the insulator, and β_s is the Schottky constant:

$$\beta_s = \left(\frac{q^3}{4\pi\varepsilon\varepsilon_0}\right),$$

q is the charge of the electron, k is the Boltzmann constant, T is the absolute temperature, ε_0 is the permittivity of the free space, and ε ~5.5 is the high-frequency dielectric constant for ferroelectric ceramics.

Analysis of *I-V* characteristics at room temperature shows that experimental values of the slopes determined for the Schottky model exceed the calculated values on average by 3.65 times. Somewhat better results were obtained for the Poole-Frenkel model, where the discrepancy between calculated and experimental slopes was ~ 1.8 times. However, the Simmons model allowed for a much better agreement, with the theoretical values and the ratios of the experimental and calculated slopes being in the range from 0.7 to 1.5.

Approximation of *I-V* characteristics with a power law resulted in the exponent m, which varied for different part types over a wide range (from 2 to 5) at room temperature. However, at high temperatures (from 125 °C to 180 °C) different capacitors had close values of m ~ 1.5. This type of *I-V* characteristics can be attributed to SCLC in the case of injection from pointed electrodes. Lee et al. [5] and Burton [10] observed near 3/2 power dependence of currents on voltage for Z5U and X7R capacitors. The results were explained by electron emission from electrode protuberances and asperities that considered a dominant cause of leakage currents in MLCCs. The presence of electrode protuberances in their work was confirmed by cross section and scanning electron microscopy (SEM) that indicated the irregular nature of electrodes.

Our cross-sectional examinations did not reveal substantial irregularities in the electrodes, and considering that the same *I-V* characteristics were observed for parts from different manufacturers, it appears more likely that the 3/2 law is due to some intrinsic irregularities in the distribution of the electric field caused by the micro-grain structure of ceramic materials. Grains that have greater conductivity compared to the shells [17] might play a role of virtual electrodes operating effectively as point contacts for electron injection.

All models predict Arrhenius-like temperature dependence and the values of E_a, calculated at relatively low voltages for different part types, vary from 0.55 eV to 1.1 eV. These values are lower than the values reported for X7R capacitors by Lee, Burton, et al. [5, 10], from 1.2 eV to 1.3 eV.

C. Leakage currents caused by mechanical defects.

Based on the results presented in this work, crack-related leakage currents, in most cases, are below or comparable with the intrinsic leakage currents; so even measurements taken after hours of electrification might not reveal cracks in large value, low-voltage ceramic capacitors. Although voltage and temperature dependence of the damage-related leakage currents is not known, this dependence is most likely less strong compared to the intrinsic leakage currents. For this reason, attempts to screen-out damaged capacitors by IR measurements at high voltages and/or temperatures are not effective.

D. IR measurements based on absorption voltages.

For normal quality capacitors, intrinsic leakage currents at temperatures below 85 °C increase with voltage exponentially, according to the Simpson equation (6). Considering that the voltage dependence of the crack-related component of currents is less significant, to avoid the masking effect by the intrinsic leakage currents, the measurements should be made at low voltages. However, leakage currents at low voltages are extremely small and cannot be measured accurately enough. In this regard, measurements of time dependence of absorption voltages that do not exceed a few volts and are determined by integrals of the leakage currents provide an effective mean for discrimination of normal and fractured capacitors.

Testing of more than 20 part types showed that the standard IR measurements that are based on 2 minutes of electrification failed to reveal fractured parts in all cases. Even long-term (1 hour) electrification was effective in only 35% of the cases, which is still two-times less than the IR_{abs} measurements that were effective in more than 70% of the cases.

E. Effect of absorption voltages on low-voltage failures in MLCCs.

The presence of a relatively low voltage across the capacitors during storage might initiate degradation processes similar to those that cause failures in capacitors with defects during low-voltage humidity testing. Several cases of failures in ceramic capacitors after long-term storage have been reported. Holladay [19] observed failures in a group of 100 capacitors stored on the shelf for 2 years at room ambient. These parts had IR ~15 kohm at 2V, but the value jumped to ~300 Mohm at 16V, which is typical for the low-voltage failure phenomenon. Three out of 30 virgin CDR31BP470BJMS capacitors from a lot suspected to be defective and causing failures in hybrids were found “leaky” during initial testing [20]. Assuming that initially all these MIL-spec parts were normal, the observed 10% failures can be ascribed as storage-induced failures. Several cases of failures in MLCCs were observed during unbiased testing at 85°C/85% RH. It is possible that although capacitors were not biased, absorption voltages have created conditions similar to low-voltage humidity testing.

IX. Conclusion

1. Currents in MLCCs after application of a step voltage are a sum of charging, absorption, and leakage currents. At room temperatures, the first component prevails during initial moments, up to ~ 1 sec, the second up to several hours, and the third, which is sensitive to the presence of defects, might be revealed after several hours of polarization.
2. Absorption currents in capacitors follow the Curie van Schwendler power law, with the exponent varying from 0.6 to 1.3. Polarization and depolarization currents are reproducible, have opposite polarity, and their isochronic values are similar. Absorption currents are not sensitive to the presence of cracks, have a weak dependence on temperature, increase linearly with voltage up to 2 to 3 times VR, and stabilize at larger voltages.
3. Absorption processes in MLCCs can be explained by electron trapping in states at the metal/ceramic interface, as a result of tunneling. Absorption capacitance increases with the nominal value of capacitance, and is on average ~30% of the nominal value. The effective concentration of the interface traps is in the range from 1.8×10^{13} cm^{-2} to 6×10^{13} cm^{-2}.
4. At low temperatures, intrinsic leakage currents in MLCCs can be described using the Schottky model with Simmons corrections. At temperatures above 85 °C, *I-V* characteristics follow a power law, $I \sim V^m$, where m is a constant close to 1.5. Activation energy of leakage currents at low voltages for different types of X7R capacitors is in the range from 0.55 eV to 1.1 eV and decreases with voltage.

5. Absorption voltages in X7R MLCCs, after 1-hour of polarization at VR and a brief short circuit, typically exceed 1 or 2 volts in a few hours and remain above 1 V even after hundreds of hours of storage at room conditions. The maximum value of V_{abs} does not correlate with the value of capacitance, increases with the duration and voltage of polarization, and appears to stabilize at voltages exceeding 2 to 3 times the rated voltage.

6. A simple model that is based on the Dow equivalent circuit for capacitors with absorption has been developed to explain long-term variations of absorption voltages and estimate insulation resistances in MLCCs. The time to roll-off of absorption voltages and the rate of voltage decrease are related to the leakage currents in the capacitors. This allows for estimations of the insulation resistances at low voltages and discrimination between normal and fractured capacitors.

X. Acknowledgment

This work was sponsored by NASA Electronic Parts and Packaging (NEPP) program. The author is thankful to Michel Sampson, NEPP Program Manager, for support of this investigation, and to Jaemi Herzberger (UMCP) for assistance with preparing the manuscript.

XI. References

[1] A. Teverovsky, "Breakdown Voltages in Ceramic Capacitors with Cracks," *IEEE Transactions on Dielectrics and Electrical Insulation,* vol. 19, pp. 1448-1455, 2012.

[2] G. G. Raju, "*Dielectrics in electric fields*": CRC Press, Marcel Dekker, p.^pp. 592, 2003.

[3] X. Xu, M. Niskala, A. Gurav, M. Laps, and K. Saarinen, "Advances in Class-I C0G MLCC and SMD Film Capacitors," in *The 28th symposium for passive components, CARTS'07*, Newport Beach, CA, 2008.

[4] H. Bachhofer, H. Reisinger, H. Schroeder, T. Haneder, C. Dehm, H. Von Philipsborn, and R. Waser, "Relaxation effects and steady-state conduction in non-stoichiometric SBT films," *Integrated Ferroelectrics,* vol. 33, pp. 245-252, 2001.

[5] H. Y. Lee, K. C. Lee, J. N. Schunke, and L. C. Burton, "Leakage currents in multilayer ceramic capacitors," *IEEE Transactions on Components Hybrids and Manufacturing Technology,* vol. 7, pp. 443-453, 1984.

[6] H. Kliem, "Kohlrausch relaxations: new aspects about the everlasting story," *Dielectrics and Electrical Insulation, IEEE Transactions on,* vol. 12, pp. 709-718, 2005.

[7] J. C. Kuenen and G. C. M. Meijer, "Measurement of dielectric absorption of capacitors and analysis of its effects on VCOs," *Instrumentation and Measurement, IEEE Transactions on,* vol. 45, pp. 89-97, 1996.

[8] A. Teverovsky, "Thermal Shock Testing and Fracturing of MLCCs under Manual Soldering Conditions," *IEEE Transactions on Device and Materials Reliability* vol. 12, pp. 413-419, 2012.

[9] P. C. Dow, "An Analysis of Certain Errors in Electronic Differential Analyzers II-Capacitor Dielectric Absorption," *Electronic Computers, IRE Transactions on,* vol. EC-7, pp. 17-22, 1958.

[10] L. C. Burton, "Intrinsic mechanisms of multilayer ceramic capacitor failure," Virginia Polytechnic Inst. and State Univ., Blacksburg, VA, ADA199113, 1998, pp. 1-57.

[11] J. H. Koh, B. M. Moon, and A. Grishin, "Dielectric properties and Schottky barriers in silver tantalate-niobate thin film capacitors," *Integrated Ferroelectrics,* vol. 39, pp. 1361-1368, 2001.

[12] L. Pintilie, I. Vrejoiu, D. Hesse, G. LeRhun, and M. Alexe, "Ferroelectric polarization-leakage current relation in high quality epitaxial Pb(Zr, Ti)O-3 films," *Physical Review B,* vol. 75, Mar 2007.

[13] J. C. Shin, J. Park, C. S. Hwang, and H. J. Kim, "Dielectric and electrical properties of sputter grown (Ba,Sr)TiO3 thin films," *JOURNAL OF APPLIED PHYSICS,* vol. 86, pp. 506-513, Jul 1999.

[14] E. Loh, "A model of dc leakage in ceramic capacitors," *Journal of Applied Physics,* vol. 53, pp. 6229-6235, 1982.

[15] P. Zubko, D. J. Jung, and J. F. Scott, "Electrical characterization of PbZr0.4Ti0.6O3 capacitors," *Journal of applied physics,* vol. 100, Dec 2006.

[16] F. D. Morrison, P. Zubko, D. J. Jung, J. F. Scott, P. Baxter, M. M. Saad, R. M. Bowman, and J. M. Gregg, "High-field conduction in barium titanate," *Applied Physics Letters,* vol. 86, Apr 2005.

[17] M. Dawber, K. M. Rabe, and J. F. Scott, "Physics of thin-film ferroelectric oxides," *Reviews of Modern Physics,* vol. 77, pp. 1083-1130, Oct 2005.

[18] J. G. Simmons, "Richardson-Schottky effect in solids," *Physical Review Letters,* vol. 15, pp. 967-968, 1965.

[19] A. M. Holladay, "Unstable insulation resistance in ceramic capacitors " *Proceedings of Capacitor Technologies, Applications and Reliability, NASA,* pp. 27-31, 1981.

[20] M. Sampson, J. Brusse, and A. Teverovsky, "Humidity Steady State Low Voltage Testing of MLCCs (Based on NESC Technical Assessment Report)," in *CARTS USA*, Jacksonville, Fl, 2011.